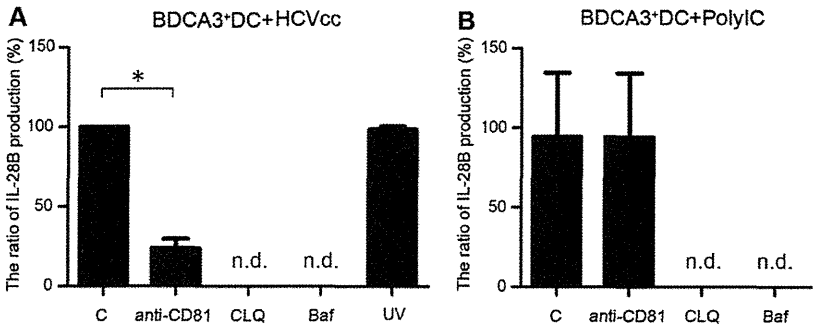

Fig. 5. The CD81 and endosome acidification is involved in the production of IL-28B from HCV-stimulated BDCA3$^+$ DCs, but HCV replication is not necessary. (A,B) BDCA3$^+$ DCs were cultured at 2.5 $\times$ 10^4 cells with HCVcc at an MOI of 10 (A) or poly IC (25 μg/mL) (B). In some experiments, UV-irradiated HCVcc was used at the same MOI, and BDCA3$^+$ DCs were treated with anti-CD81Ab (5 mg/mL), chloroquine (10 mM), or bafilomycin A1 (25 nM). The results are expressed as ratios of IL-28B quantity with or without the treatments. They are shown as mean $\pm$ SEM from five experiments. *$P < 0.05$ by paired t test. C, control; CLQ, treatment with chloroquine; Baf, treatment with bafilomycin A1; UV, ultraviolet-irradiated HCVcc; n.d., not detected.

CD81 and Endosome Acidification Are Involved in IL-28B Production from HCV-Stimulated BDCA3$^+$ DCs, but HCV Replication Is Not Involved. It is not known whether HCV entry and subsequent replication in DCs is involved or not in IFN response.[18,19] To test this, BDCA3$^+$ DCs were inoculated with UV-irradiated, replication-defective HCVcc. We confirmed that UV exposure under the current conditions is sufficient to negate HCVcc replication in Huh7.5.1 cells, as demonstrated by the lack of expression of NS5A after inoculation (data not shown). BDCA3$^+$ DCs produced comparable levels of IL-28B with UV-treated HCVcc, indicating that active HCV replication is not necessary for IL-28B production (Fig. 5A).

We next examined whether or not the association of HCVcc with BDCA3$^+$ DCs by CD81 is required for IL-28B production. It has been reported that the E2 region of HCV structural protein is associated with CD81 on cells when HCV enters susceptible cells.[13,20] We confirmed that all DC subsets express CD81, the degree of which was most significant on BDCA3$^+$ DCs (Fig. 1B, Fig. S1). Masking of CD81 with Ab significantly impaired IL-28B production from HCVcc-stimulated BDCA3$^+$ DCs in a dose-dependent manner (Fig. 5A, Fig. S8), suggesting that HCV-E2 and CD81 interaction is involved in the induction. The treatment of poly IC-stimulated BDCA3$^+$ DCs with anti-CD81 Ab failed to suppress IL-28B production (Fig. 5B).

HCV enters the target cells, which is followed by fusion steps within acidic endosome compartments. Chloroquine and bafilomycin A1 are well-known and broadly used inhibitors of endosome TLRs, which are reported to be capable of blocking TLR3 response in human monocyte-derived DC.[21,22] In our study, the treatment of BDCA3$^+$ DCs with chloroquine, bafilomycin A1, or NH4Cl significantly suppressed their IL-28B production either in response to HCVcc or poly IC (Fig. 5A,B, NH4Cl, data not shown). These results suggest that the endosome acidification is involved in HCVcc- or poly IC-stimulated BDCA3$^+$ DCs to produce IL-28B. The similar results were obtained with HCVcc-stimulated pDCs for the production of IL-28B (Fig. S9). We validated that such concentration of chloroquine (10 mM) and bafilomycin A1 (25 nM) did not reduce the viability of BDCA3$^+$ DCs (Fig. S10).

BDCA3$^+$ DCs Produce IL-28B in Response to HCVcc by a TIR-Domain-Containing Adapter-Inducing Interferon-β (TRIF)-Dependent Mechanism. TRIF/TICAM-1, a TIR domain-containing adaptor, is known to be essential for the TLR3-mediated pathway.[23] In order to elucidate whether TLR3-dependent pathway is involved or not in IL-28B response of BDCA3$^+$ DCs, we added the cell-permeable TRIF-specific inhibitory peptide (Invivogen) or the control peptide to poly IC- or HCVcc-stimulated BDCA3$^+$ DCs. Of particular interest, the TRIF-specific inhibitor peptide, but not the control one, significantly suppressed IL-28B production from poly IC- or HCVcc-stimulated BDCA3$^+$ DCs (Fig. 6A,B). In clear contrast, the TRIF-specific inhibitor failed to suppress IL-28B from HCVcc-stimulated pDCs (Fig. 6C), suggesting that pDCs recognize HCVcc in an endosome-dependent but TRIF-independent pathway. These results show that BDCA3$^+$ DCs may recognize HCVcc by way of the TRIF-dependent pathway to produce IL-28B.

BDCA3$^+$ DCs in Subjects with IL-28B Major Genotype Produce More IL-28B in Response to HCV than Those with IL-28B Minor Type. In order to compare the ability of BDCA3$^+$ DCs to release IL-28B in healthy subjects between IL28B major (rs8099917, TT)

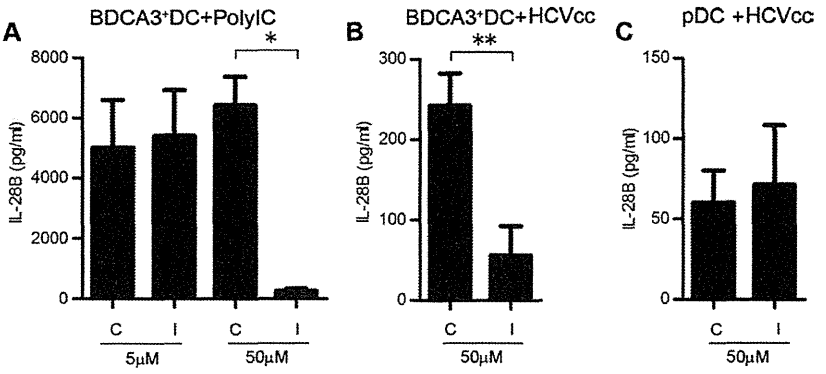

Fig. 6. BDCA3$^+$ DCs produce IL-28B upon HCVcc stimulation in a TRIF-dependent mechanism. BDCA3$^+$ DCs or pDCs had been treated with 5 or 50 mM TRIF inhibitory peptide or control peptide for 2 hours. Subsequently, BDCA3$^+$ DCs were stimulated with Poly IC (25 μg/mL) or HCVcc (MOI = 10), and pDCs were stimulated with HCVcc (MOI = 10), respectively. IL-28B was quantified by ELISA. They are shown as mean ± SEM from five experiments. *$P < 0.05$ by paired t test. C, TRIF control peptide; I, TRIF inhibitory peptide.

and minor hetero (TG) genotypes, we stimulated BDCA3$^+$ DCs of the identical subjects with poly IC (25 mg/mL, 2.5 mg/mL, 0.25 mg/mL), HCVcc or JFH-1-infected Huh 7.5.1, and subjected them to ELISA. The levels of IL-28B production by poly IC-stimulated BDCA3$^+$ DCs were comparable between subjects with IL-28B major and minor type (Fig. 7A). Similar results were obtained with the lesser concentrations of poly IC (Fig. S11). Of particular interest, in response to HCVcc or JFH-1 Huh7.5.1 cells, the levels of IL-28B from BDCA3$^+$ DCs were significantly higher in subjects with IL-28B major than those with minor type (Fig. 7B,C, S12).

Discussion

In this study we demonstrated that human BDCA3$^+$ DCs (1) are present at an extremely low frequency in PBMC but are accumulated in the liver; (2) are capable of producing IL-29/IFN-λ1, IL-28A/IFN-λ2, and IL-28B/IFN-λ3 robustly in response to HCV; (3) recognize HCV by a CD81-, endosome acidification and TRIF-dependent mechanism; and (4) produce larger amounts of IFN-λs upon HCV stimulation in subjects with IL-28B major genotype (rs8099917, TT). These characteristics of BDCA3$^+$ DCs are quite unique in comparison with other DC repertoires in the settings of HCV infection.

At the steady state, the frequency of DCs in the periphery is relatively lower than that of the other immune cells. However, under disease conditions or physiological stress, activated DCs dynamically migrate to the site where they are required to be functional. However, it remains obscure whether functional BDCA3$^+$ DCs exist or not in the liver. We identified BDCA3$^+$CLEC9A$^+$ cells in the liver tissue (Fig. 1D). In a paired frequency analysis of BDCA3$^+$ DCs between in PBMCs and in IHLs, the cells are more abundant in the liver. The phenotypes of liver BDCA3$^+$ DCs were more mature than the PBMC counterparts. In support of our observations, a recent publication showed that CD141$^+$ (BDCA3$^+$) DCs are accumulated and more mature in the liver, the trend of which is more in HCV-infected liver.[24] We confirmed that liver BDCA3$^+$ DCs are functional, capable of releasing IFN-λs in response to poly IC or HCVcc.

BDCA3$^+$ DCs were able to produce large amounts of IFN-λs but much less IFN-β or IFN-α upon TLR3 stimulation. In contrast, in response to TLR9 agonist,

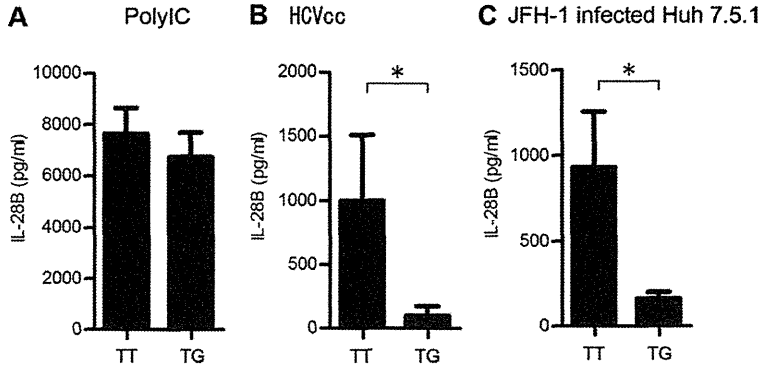

Fig. 7. In response to HCVcc, BDCA3$^+$ DCs of healthy donors with IL-28B major genotype (rs8099917, TT) produced more IL-28B than those with minor type (TG). BDCA3$^+$ DCs of healthy donors with IL-28B TT (rs8099917) or TG genotype were cultured at 2.5 × 10^4 cells with 25 mg/mL poly IC (A), with HCVcc at an MOI of 10 (B), or with JFH-1-infected Huh 7.5.1 cells (C) for 24 hours. The supernatants were subjected to IL-28B ELISA. The same healthy donors were examined for distinct stimuli. The results are the mean ± SEM from 15 donors with TT and 8 with TG, respectively. *$P < 0.05$ by Mann-Whitney U test.

pDCs released large amounts of IFN-β and IFN-α but much less IFN-λs. Such distinctive patterns of IFN response between BDCA3$^+$ DCs and pDCs are of particular interest. It has been reported that interferon regulatory factor (IRF)-3, IRF-7, or nuclear factor kappa B (NF-κB) are involved in IFN-β and IFN-λ1, while IRF-7 and NF-κB are involved in IFN-α and IFN-λ2/λ3.[5] Presumably, the stimuli with TLR3/retinoic acid-inducible gene-I (RIG-I) (poly IC) or TLR9 agonist (CpG-DNA) in DCs are destined to activate these transcription factors, resulting in the induction of both types of IFN at comparable levels. However, the results of the present study did not agree with such overlapping transcription factors for IFN-λs, IFN-β, and IFN-α. Two possible explanations exist for different levels of IFN-λs and IFN-α production by BDCA3$^+$ DCs and pDCs. First, the transcription factors required for full activation of IFN genes may differ according to the difference of DC subsets. The second possibility is that since type III IFN genes have multiple exons, they are potentially regulated by post-transcriptional mechanisms. Thus, it is possible that such genetic and/or posttranscriptional regulation is distinctively executed between BDCA3$^+$ DCs and pDCs. Comprehensive analysis of gene profiles downstream of TLRs or RIG-I in BDCA3$^+$ DCs should offer some information on this important issue.

BDCA3$^+$ DCs were found to be more sensitive to HCVcc than JEV or HSV in IL-28B/IFN-λ3 production. Such different strengths of IL-28B in BDCA3$^+$ DCs depending on the virus suggest that different receptors are involved in virus recognition. Again, the question arises of why BDCA3$^+$ DCs produce large amounts of IFN-λs compared to the amounts produced by pDCs in response to HCVcc. Considering that IRF-7 and NF-κB are involved in the transcription of the IL-28B gene, it is possible that BDCA3$^+$ DCs successfully activate both transcription factors upon HCVcc for maximizing IL-28B, whereas pDCs fail to do so. In support for this possibility, in pDCs it is reported that NF-κB is not properly activated upon HCVcc or hepatoma cell-derived HCV stimulations.[25]

In the present study we demonstrated that HCV entry into BDCA3$^+$ DCs through CD81 and subsequent endosome acidification are critically involved in IL-28B responses. Involvement of TRIF-dependent pathways in IL-28B production was shown by the significant inhibition of IL-28B with TRIF inhibitor. Nevertheless, active HCV replication in the cells is not required. Based on our data, we considered that BDCA3$^+$ DCs recognize HCV genome mainly by an endosome and TRIF-dependent mechanism. Although the results with UV-irradiated HCVcc, anti-CD81 blocking Ab, and chloroquine were quite similar, the TRIF-specific inhibitor failed to suppress IL-28B from pDCs (Fig. 6, Fig. S9).

In the coculture with JFH-transfected Huh7.5.1 cells, BDCA3$^+$ DCs presumably receive some signals for IL-28B production by way of cell-to-cell dependent and independent mechanisms. In the present study, most of the stimuli to BDCA3$^+$ DCs for IL-28B production may be the released HCVcc from Huh7.5.1 cells, judging from the inability of suppression with transwells. However, a contribution of contact-dependent mechanisms cannot be excluded in the coculture experiments. HCV genome is transmissible from infected hepatocytes to uninfected ones through tight junction molecules, such as claudin-1 and occuludin. Further investigation is needed to clarify whether such cell-to-cell transmission of viral genome is operated or not in BDCA3$^+$ DCs.

The relationship between IL-28B expression and the induction of ISGs has been drawing much research attention. In primary human hepatocytes, it is reported that HCV primarily induces IFN-λ, instead of type-I IFNs, subsequently enhancing ISG expression.[7] Of particular interest is that the level of hepatic IFN-λs is closely correlated with the strength of ISG response.[26] These reports strongly suggest that hepatic IFN-λs are a crucial driver of ISG induction and subsequent HCV eradication. Besides, it is likely that BDCA3$^+$ DCs, as a bystander IFN-λ producer in the liver, have a significant impact on hepatic ISG induction. In support of this possibility, we demonstrated in this study that BDCA3$^+$ DCs are capable of producing large amounts of IFN-λs in response to HCV, thereby inducing ISGs in the coexisting liver cells.

Controversial results have been reported regarding the relationship between IL28B genotypes and the levels of IL-28 expression. Nevertheless, in chronic hepatitis C patients with IL-28B major genotype, the IL-28 transcripts in PBMCs are reported to be higher than those with minor genotype.[2] In this study, by focusing on a prominent IFN-λ producer (BDCA3$^+$ DCs) and using the assay specific for IL-28B, we showed that the subjects with IL-28B major genotype could respond to HCV by releasing more IL-28B. Of interest, such a superior capacity of BDCA3$^+$ DCs was observed only in response to HCV but not to poly IC. Since the pathways downstream of TLR3-TRIF leading to IL-28B in BDCA3$^+$ DCs should be the same, either HCV or poly IC stimulation, two plausible explanations exist for such a distinct IL-28B response. First, it is possible that distinct epigenetic regulation may be

involved in IL-28B gene according to the IL-28B genotypes. Recently, in influenza virus infection, it is reported that micro-RNA29 and DNA methyltransferase are involved in the cyclooxygenase-2-mediated enhancement of IL-29/IFN-λ1 production.[27] This report supports the possibility that similar epigenetic machineries could be operated as well in HCV-induced IFN-λs production. Second, it is plausible that the efficiency of the stimulation of TLR3-TRIF may be different between the IL-28B genotypes. Since HCV reaches endosome in BDCA3$^+$ DCs by way of the CD81-mediated entry and subsequent endocytosis pathways, the efficiencies of HCV handling and enzyme reactions in endosome may be influential in the subsequent TLR3-TRIF-dependent responses. Certain unknown factors regulating such process may be linked to the IL-28B genotypes. For a comprehensive understanding of the biological importance of IL-28B in HCV infection, such confounding factors, if they exist, need to be explored.

In conclusion, human BDCA3$^+$ DCs, having a tendency to accumulate in the liver, recognize HCV and produce large amounts of IFN-λs. An enhanced IL-28B/IFN-λ3 response of BDCA3$^+$ DCs to HCV in subjects with IL-28B major genotype suggests that BDCA3$^+$ DCs are one of the key players in anti-HCV innate immunity. An exploration of the molecular mechanisms of potent and specialized capacity of BDCA3$^+$ DCs as IFN-λ producer could provide useful information on the development of a natural adjuvant against HCV infection.

References

1. Suppiah V, Moldovan M, Ahlenstiel G, Berg T, Weltman M, Abate ML, et al. IL28B is associated with response to chronic hepatitis C interferon-alpha and ribavirin therapy. Nat Genet 2009;41:1100-1104.
2. Tanaka Y, Nishida N, Sugiyama M, Kurosaki M, Matsuura K, Sakamoto N, et al. Genome-wide association of IL28B with response to pegylated interferon-alpha and ribavirin therapy for chronic hepatitis C. Nat Genet 2009;41:1105-1109.
3. Ge D, Fellay J, Thompson AJ, Simon JS, Shianna KV, Urban TJ, et al. Genetic variation in IL28B predicts hepatitis C treatment-induced viral clearance. Nature 2009;461:399-401.
4. Thomas DL, Thio CL, Martin MP, Qi Y, Ge D, O'Huigin C, et al. Genetic variation in IL28B and spontaneous clearance of hepatitis C virus. Nature 2009;461:798-801.
5. Kotenko SV. IFN-lambdas. Curr Opin Immunol 2011;23:583-590.
6. Urban TJ, Thompson AJ, Bradrick SS, Fellay J, Schuppan D, Cronin KD, et al. IL28B genotype is associated with differential expression of intrahepatic interferon-stimulated genes in patients with chronic hepatitis C. Hepatology 2010;52:1888-1896.
7. Park H, Serti E, Eke O, Muchmore B, Prokunina-Olsson L, Capone S, et al. IL-29 is the dominant type III interferon produced by hepatocytes during acute hepatitis C virus infection. Hepatology 2012;56:2060-2070.
8. Medzhitov R. Recognition of microorganisms and activation of the immune response. Nature 2007;449:819-826.
9. Liu YJ. Dendritic cell subsets and lineages, and their functions in innate and adaptive immunity. Cell 2001;106:259-262.
10. Poulin LF, Salio M, Griessinger E, Anjos-Afonso F, Craciun L, Chen JL, et al. Characterization of human DNGR-1+ BDCA3+ leukocytes as putative equivalents of mouse CD8alpha+ dendritic cells. J Exp Med 2010;207:1261-1271.
11. Lauterbach H, Bathke B, Gilles S, Traidl-Hoffmann C, Luber CA, Fejer G, et al. Mouse CD8alpha+ DCs and human BDCA3+ DCs are major producers of IFN-lambda in response to poly IC. J Exp Med 2010;207:2703-2717.
12. Wakita T, Pietschmann T, Kato T, Date T, Miyamoto M, Zhao Z, et al. Production of infectious hepatitis C virus in tissue culture from a cloned viral genome. Nat Med 2005;11:791-796.
13. Lindenbach BD, Evans MJ, Syder AJ, Wolk B, Tellinghuisen TL, Liu CC, et al. Complete replication of hepatitis C virus in cell culture. Science 2005;309:623-626.
14. Mori Y, Okabayashi T, Yamashita T, Zhao Z, Wakita T, Yasui K, et al. Nuclear localization of Japanese encephalitis virus core protein enhances viral replication. J Virol 2005;79:3448-3458.
15. Sugiyama M, Kimura T, Naito S, Mukaide M, Shinauchi T, Ueno M, et al. Development of interferon lambda 3 specific quantification assay for its mRNA and serum/plasma specimens. Hepatol Res 2012;42:1089-1099.
16. Schreibelt G, Klinkenberg LJ, Cruz LJ, Tacken PJ, Tel J, Kreutz M, et al. The C type lectin receptor CLEC9A mediates antigen uptake and (cross-)presentation by human blood BDCA3+ myeloid dendritic cells. Blood 2012;119:2284-2292.
17. Jongbloed SL, Kassianos AJ, McDonald KJ, Clark GJ, Ju X, Angel CE, et al. Human CD141+ (BDCA-3)+ dendritic cells (DCs) represent a unique myeloid DC subset that cross-presents necrotic cell antigens. J Exp Med 2010;207:1247-1260.
18. Marukian S, Jones CT, Andrus L, Evans MJ, Ritola KD, Charles ED, et al. Cell culture-produced hepatitis C virus does not infect peripheral blood mononuclear cells. Hepatology 2008;48:1843-1850.
19. Liang H, Russell RS, Yonkers NL, McDonald D, Rodriguez B, Harding CV, et al. Differential effects of hepatitis C virus JFH1 on human myeloid and plasmacytoid dendritic cells. J Virol 2009;83:5693-5707.
20. Zhang J, Randall G, Higginbottom A, Monk P, Rice CM, McKeating JA. CD81 is required for hepatitis C virus glycoprotein-mediated viral infection. J Virol 2004;78:1448-1455.
21. Blanchard E, Belouzard S, Goueslain L, Wakita T, Dubuisson J, Wychowski C, et al. Hepatitis C virus entry depends on clathrin-mediated endocytosis. J Virol 2006;80:6964-6972.
22. de Bouteiller O, Merck E, Hasan UA, Hubac S, Benguigui B, Trinchieri G, et al. Recognition of double-stranded RNA by human toll-like receptor 3 and downstream receptor signaling requires multimerization and an acidic pH. J Biol Chem 2005;280:38133-38145.
23. Takeda K, Akira S. TLR signaling pathways. Semin Immunol 2004;16:3-9.
24. Velazquez VM, Hon H, Ibegbu C, Knechtle SJ, Kirk AD, Grakoui A. Hepatic enrichment and activation of myeloid dendritic cells during chronic hepatitis C virus infection. Hepatology 2012;56:2071-2081.
25. Dental C, Florentin J, Aouar B, Gondois-Rey F, Durantel D, Baumert TF, et al. Hepatitis C virus fails to activate NF-kappaB signaling in plasmacytoid dendritic cells. J Virol 2012;86:1090-1096.
26. Thomas E, Gonzalez VD, Li Q, Modi AA, Chen W, Noureddin M, et al. HCV infection induces a unique hepatic innate immune response associated with robust production of type III interferons. Gastroenterology 2012;142:978-988.
27. Fang J, Hao Q, Liu L, Li Y, Wu J, Huo X, Zhu Y. Epigenetic changes mediated by microRNA miR29 activate cyclooxygenase 2 and lambda-1 interferon production during viral infection. J Virol 2012;86:1010-1020.

JVI
Journals.ASM.org

Ifit1 Inhibits Japanese Encephalitis Virus Replication through Binding to 5′ Capped 2′-O Unmethylated RNA

Taishi Kimura,[a,b] Hiroshi Katoh,[d] Hisako Kayama,[a,b,f] Hiroyuki Saiga,[a] Megumi Okuyama,[a] Toru Okamoto,[d] Eiji Umemoto,[a,b,f] Yoshiharu Matsuura,[d] Masahiro Yamamoto,[c,e] Kiyoshi Takeda[a,b,f]

Department of Microbiology and Immunology, Graduate School of Medicine,[a] Laboratory of Mucosal Immunology,[b] and Laboratory of Immunoparasitology,[c] WPI Immunology Frontier Research Center, Osaka University, Osaka, Japan; Department of Molecular Virology[d] and Department of Immunoparasitology,[e] Research Institute for Microbial Diseases, Osaka University, Osaka, Japan; Core Research for Evolutional Science and Technology, Japan Science and Technology Agency, Saitama, Japan[f]

The interferon-inducible protein with tetratricopeptide (IFIT) family proteins inhibit replication of some viruses by recognizing several types of RNAs, including 5′-triphosphate RNA and 5′ capped 2′-O unmethylated mRNA. However, it remains unclear how IFITs inhibit replication of some viruses through recognition of RNA. Here, we analyzed the mechanisms by which Ifit1 exerts antiviral responses. Replication of a Japanese encephalitis virus (JEV) 2′-O methyltransferase (MTase) mutant was markedly enhanced in mouse embryonic fibroblasts and macrophages lacking Ifit1. Ifit1 bound 5′-triphosphate RNA but more preferentially associated with 5′ capped 2′-O unmethylated mRNA. Ifit1 inhibited the translation of mRNA and thereby restricted the replication of JEV mutated in 2′-O MTase. Thus, Ifit1 inhibits replication of MTase-defective JEV by inhibiting mRNA translation through direct binding to mRNA 5′ structures.

mRNA has a 5′ cap structure, in which the N-7 position of the guanosine residue is methylated. The 5′ cap structure is known to be responsible for the stability and efficient translation of mRNA (1, 2). In higher eukaryotes, the first one or two 5′ nucleotides are additionally methylated at the ribose 2′-O position by distinct host nuclear 2′-O methyltransferases (MTases) (3, 4). However, the functional role of 2′-O methylation (2′-O Me) remains poorly understood. Several viruses that replicate in the cytoplasm possess their own mRNA capping machineries (5–10). For positive-stranded flaviviruses, nonstructural protein 3 (NS3) acts as an RNA 5′-triphosphatase and NS5 possesses both N-7 and 2′-O MTase activities (8, 11, 12). Recent studies have revealed that 2′-O methylation of the mRNA 5′ cap in these viruses is important for evasion from the host innate immune responses (13–15). However, the 2′-O MTase activity has been shown to be absent from several paramyxoviruses, such as Newcastle disease virus (NDV) and respiratory syncytial virus (RSV) (16, 17).

Type I interferons (IFNs) induce the expression of a large number of antiviral genes through a Janus kinase/signal transducer and activator of transcription (JAK/STAT) pathway (18, 19). Among the IFN-inducible genes, the IFN-inducible protein with tetratricopeptide (IFIT) genes comprise a large family with three (*Ifit1*, *Ifit2*, and *Ifit3*) and four (*IFIT1*, *IFIT2*, *IFIT3*, and *IFIT5*) members in mice and humans, respectively. The murine and human genes are clustered in loci on chromosomes 19C1 and 10q23, respectively (20). IFIT family proteins reportedly associate with several host proteins to exert various cellular functions (21, 22). For example, human IFIT1/IFIT2 and murine Ifit1/Ifit2 bind to eukaryotic translational initiation factor 3 (eIF3) subunits to inhibit translation (23–26). IFIT1 has been suggested to interact with STING/MITA to negatively regulate IRF3 activation (27), whereas IFIT3 may bind TBK1 to enhance type I IFN production and with JAB1 to inhibit leukemia cell growth (28, 29).

In addition to binding host factors, IFIT proteins have functional effects by interacting directly with products of viruses. Human IFIT1 interacts with the human papillomavirus E1 protein and human IFIT2 interacts with the AU-rich RNA of NDV to exert antiviral effects (30, 31). Direct binding of IFIT proteins to virus RNA has also been demonstrated in several recent studies. IFIT1 and IFIT5 bind to the 5′-triphosphate (5′-PPP) RNA that is present in the genomes of viruses (32, 33). Structural studies of human IFIT2 and human IFIT5 identified an RNA-binding site and defined the structural basis of a complex with 5′-PPP RNA (31, 33). However, these structural studies did not explain how IFIT binds to or restricts virus RNA that has a 5′ cap but lacks methylation at the 2′-O position (13–15). Thus, it remains unclear how IFITs mediate antiviral activities against viruses that have a 5′ cap but lack 2′-O MTase activity.

In this study, we analyzed the mechanisms by which murine Ifit1 exerts the host defense against a flavivirus lacking 2′-O MTase activity. Ifit1 was found to preferentially interact with 5′ capped mRNA without 2′-O methylation and inhibit its translation. Thus, Ifit1 participates in antiviral responses targeting 5′ capped mRNA without 2′-O methylation.

MATERIALS AND METHODS

Mice. All animal experiments were conducted in accordance with the guidelines of the Animal Care and Use Committee of the Graduate School of Medicine, Osaka University. The gene-targeting strategies for generating *Ifit1*-knockout (*Ifit1*$^{-/-}$) mice were described previously (34). The *Ifit1*-targeting vector was designed to replace a 1.8-kb fragment encoding the exon of *Ifit1* with a neomycin resistance gene cassette (Neo). A short arm and a long arm of the homology region from the v6.5 embryonic stem (ES) cell genome were amplified by PCR. A herpes simplex virus (HSV) thymidine kinase (tk) gene was inserted into the 3′ end of the vector. After the *Ifit1*-targeting vector was electroporated into ES cells, G418 and ganciclovir doubly resistant clones were selected and screened by PCR and

Received 2 April 2013 Accepted 26 June 2013
Published ahead of print 3 July 2013
Address correspondence to Kiyoshi Takeda, ktakeda@ongene.med.osaka-u.ac.jp.

doi:10.1128/JVI.00883-13

Southern blot analysis. An ES cell clone correctly targeting *Ifit1* was microinjected into C57BL/6 mouse blastocysts. Chimeric mice were mated with female C57BL/6 mice, and heterozygous F1 progenies were intercrossed to obtain *Ifit1*$^{-/-}$ mice.

Cells. HEK293T cells, Vero cells, and mouse embryonic fibroblasts (MEFs) were maintained in Dulbecco's modified Eagle's medium (Nakalai Tesque) supplemented with 10% fetal bovine serum (JRH Bioscience), 100 U/ml penicillin, and 100 μg/ml streptomycin (Gibco). MEFs were prepared from wild-type (WT) and *Ifit1*$^{-/-}$ day 14.5 embryos and immortalized by introduction of a plasmid encoding the simian virus 40 large T antigen. MEFs stably expressing Ifit1 were established by the previously described method with some modifications (34). In short, full-length cDNA of *Ifit1* was cloned into pMRX-puro (pMRX/*Ifit1*). Retrovirus was produced by introduction of pMRX/*Ifit1* into Plat-E packaging cells (35). MEFs were infected with the retrovirus, cultured in the presence of 1 μg/ml of puromycin (Sigma) for 5 days, and harvested for subsequent studies. To isolate peritoneal macrophages, mice were intraperitoneally injected with 5 ml of 4% thioglycolate medium (Sigma), and peritoneal exudative cells were isolated from the peritoneal cavity at 3 days postinjection. The cells were incubated for 2 h and then washed three times with Hanks' balanced salt solution. The remaining adherent cells were used as peritoneal macrophages in the experiments.

Viruses. Japanese encephalitis virus (JEV) strain AT31 (36) was used for the experiments. An NS5 K61A mutation of JEV was introduced into pMWATG1 (37) by PCR-based mutagenesis with the primers 5′-GCGAGGCTCAGCAGCTCTCCGTTGGCTCG-3′ and 5′-CGAGCCAACGGAGAGCTGCTGAGCCTCGC-3′ (the mutagenesis site is underlined) and verified by DNA sequencing. A recombinant virus, the JEV K61A mutant, was generated from pMWJEATG1/JEV K61A as previously described (36). MEFs or macrophages were infected with JEV at specified multiplicities of infection (MOIs). The virus yields in the culture supernatants were titrated by focus-forming assays on Vero cells and expressed as the number of focus-forming units (FFU), as previously described (38). The virus RNA accumulations in the JEV-infected cells were determined by real-time reverse transcription-PCR (RT-PCR) with primers targeting JEV NS5, normalized to the level of host GAPDH (glyceraldehyde-3-phosphate dehydrogenase), and expressed as the fold change in *Ifit1*$^{-/-}$ cells versus wild-type cells (value for wild type = 1).

Preparation of RNA. The 5′-terminal 200 nucleotides of the JEV genome were amplified by PCR using pMWATG1 (37) with the primers 5′-TAATACGACTCACTATTAGAAGTTTATCT-3′ (the T7 class II promoter sequence is underlined) and 5′-CATTACTACCCTCTTCACTCCCACTAGTGG-3′, and the luciferase reporter gene (*luc2*) was amplified using pGL4.14 (Promega) with the primers 5′-TAATACGACTCACTATAGGCCACCATGGAAGATGCCAAAAA-3′ (the T7 class III promoter sequence is underlined) and 5′-TACCACATTTGTAGAGGTTTTACTTGCTTT-3′. Subsequently, the PCR products were *in vitro* transcribed under the control of the T7 promoter with MEGAScript (Ambion). Biotin-labeled RNA was prepared by *in vitro* transcription in the presence of biotin-labeled UTP (PerkinElmer). Capped RNA substrates were produced with a ScriptCap 7-methylguanosine (m7G) capping system (Epicentre) in the presence (5′ cap positive [5′ cap$^+$]/2′-O Me positive [2′-O Me$^+$]) or absence (5′ cap$^+$/2′-O Me negative [2′-O Me$^-$]) of a ScriptCap vaccinia virus 2′-O MTase (Epicentre). ^{32}P-labeled m7GpppA-RNA substrate was prepared with a ScriptCap m7G capping system in the presence of ^{32}P-labeled GTP. A 5′ OH-RNA substrate was produced by incubating *in vitro*-transcribed RNA with calf intestinal alkaline phosphatase (CIAP) for 3 h at 37°C. All RNA substrates were purified with an RNeasy minikit (Qiagen) and stored at −80°C until use.

Real-time RT-PCR. Total RNA was isolated with the TRIzol reagent (Invitrogen), and 1 to 2 μg of RNA was reverse transcribed using Moloney murine leukemia virus reverse transcriptase (Promega) and random primers (Toyobo) after treatment with RQ1 DNase I (Promega). Real-time RT-PCR was performed in an ABI 7300 apparatus (Applied Biosystems) using a GoTaq real-time PCR system (Promega). All values were normalized by the expression of the GAPDH gene. The following primer sets were used: for the JEV NS5 gene, 5′-AACGCACATTACGCGTCCTAGAGATGA-3′ and 5′-CTAACCCAATACATCTCGTGATTGGAGTT-3′; for *Ifnb*, 5′-GGAGATGACGGAGAAGATGC-3′ and 5′-CCCAGTGCTGGAGAAATTGT-3′; for *luc2*, 5′-CCATTCTACCCACTCGAAGACG-3′ and 5′-CGTAGGTAATGTCCACCTCGA-3′; and for the GAPDH gene, 5′-CCTCGTCCCGTAGACAAAATG-3′ and 5′-TCTCCACTTTGCCACTGCAA-3′.

Recombinant proteins. Wild-type and K61A mutant JEV N-terminal NS5 (MTase domain) cDNAs were obtained by PCR using pMWATG1 with the primers 5′-GGATCCGGAAGGCCTGGGGGCAGGACGCTA-3′ and 5′-CTCGAGATGCTCAGGGTCTTTGTGCCACGT-3′. Full-length murine *Ifit1* cDNA and JEV MTase cDNA were inserted into pET-15b and pGEX-6P, respectively. pET/*Ifit1* and pGEX/JEV MTases were transformed into the *Escherichia coli* BL21(DE3) strain. Expression of the Ifit1 and JEV NS5 proteins was induced by addition of 0.5 mM isopropyl-1-thio-β-D-galactopyranoside (IPTG), and the expressed Ifit1 and JEV MTase proteins were purified using Ni^{2+}-affinity chromatography (Novagen) and glutathione-Sepharose 4B (Amersham Biosciences), respectively, according to each manufacturer's instructions. The purified protein was desalted and concentrated using an Amicon Ultra centrifugal filter unit (Millipore) and stored at −80°C until use.

***In vitro* MTase activity assay.** The MTase reaction was performed in a 20-μl reaction mixture of 50 mM Tris-HCl (pH 8.0), 6 mM KCl, 1.25 mM $MgCl_2$, and 0.5 mM *S*-adenosylmethionine (AdoMet) containing 10 nmol of ^{32}P-labeled m7GpppA-RNA substrate (JEV 5′-terminal 200 nucleotides) and 30 pmol of JEV MTase or 80 units of vaccinia virus 2′-O MTase (Epicentre) for 3 h at 37°C. The RNA was purified by passage through a postreaction cleanup column (Sigma) and digested with 10 U of nuclease P1 (Wako) in 50 mM sodium acetate overnight at 37°C. The samples were analyzed on thin-layer chromatography polyethyleneimine (PEI)-cellulose plates developed with 0.3 M ammonium sulfate.

RNA EMSAs. RNA electrophoretic mobility shift assays (EMSAs) were performed using a LightShift chemiluminescent RNA EMSA kit (Thermo Scientific) according to the manufacturer's instructions. Briefly, 0 to 20 pmol of recombinant murine Ifit1 and 2.5 pmol of *in vitro*-transcribed and biotin-labeled RNA were coincubated for 30 min at room temperature in RNA EMSA binding buffer (10 mM HEPES, pH 7.3, 20 mM KCl, 1 mM $MgCl_2$, 1 mM dithiothreitol, 0.1 μg/μl of yeast tRNA, 2% glycerol). The resulting Ifit1/RNA complexes were electrophoresed in a 7.5% native polyacrylamide gel. The separated RNAs were transferred to a positively charged nylon membrane and cross-linked at 120 mJ/cm^2 and an absorbance of 254 nm. The membrane was incubated with stabilized streptavidin-horseradish peroxidase conjugate (1:300 dilution; a component of the EMSA kit), and the bound stable peroxide was detected with luminol/enhancer solution (another component of the EMSA kit). The gel-shift band intensities were quantified using ImageJ software (National Institutes of Health).

RNA pulldown assay. For RNA pulldown assays, an expression vector for hemagglutinin (HA)-tagged murine full-length Ifit1 was transfected into HEK293T cells using Lipofectamine 2000 (Invitrogen). The *Ifit1*-transfected cells were lysed in RNA-binding buffer (10 mM HEPES, pH 7.3, 500 mM KCl, 1 mM EDTA, 2 mM $MgCl_2$, 0.1% NP-40, 0.1 μg/μl of yeast tRNA (Ambion), 1 U/ml of RNase inhibitor [Toyobo]), and the lysate (200 μg) was coincubated with 25 pmol of biotin-labeled RNA and streptavidin-agarose (Invitrogen) in RNA-binding buffer for 30 min at room temperature. The binding complexes were washed five times with RNA-binding buffer, followed by SDS-PAGE and immunoblotting with an anti-HA probe (F-7) antibody (Santa Cruz Biotechnology). The intensity of the detected Ifit1 band was quantified using ImageJ software (National Institutes of Health).

RNA immunoprecipitation. RNA immunoprecipitation was performed as described previously (38) with slight modifications. MEFs (2×10^5) stably expressing Flag-tagged Ifit1 were infected with JEV at an MOI of 1.0 and cultured for 24 h. The cells were then lysed in 500 μl of RNA

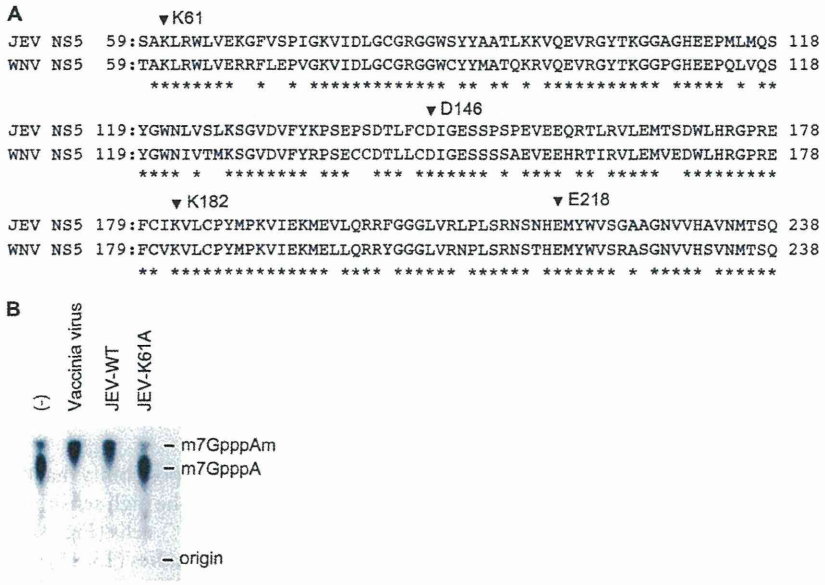

FIG 1 Generation of an MTase-defective JEV mutant. (A) Sequence homology between NS5 proteins of JEV (AT31 strain, GenBank accession number AB196926) and WNV (00-3356 strain, GenBank accession number EF530047). Arrowheads, MTase catalytic K-D-K-E tetrad; *, consensus sequences between the two proteins. (B) 2′-O MTase activity of JEV WT and JEV K61A mutant recombinant NS5 proteins by thin-layer chromatography assays. The substrate m7GpppA-RNA (^{32}P-labeled JEV 5′-terminal 200 nucleotides) was methylated *in vitro* with the respective recombinant NS5 proteins or vaccinia virus 2′-O MTase, digested with P1 nuclease, and developed on PEI-cellulose plates. The positions of 2′-O methylated (m7GpppAm) and unmethylated (m7GpppA) RNA are indicated. Data are representative of four independent experiments.

buffer (10 mM HEPES, pH 7.3, 500 mM KCl, 1 mM EDTA, 2 mM $MgCl_2$, 0.1% NP-40, 0.1 μg/μl of yeast tRNA (Ambion), 1 U/ml of RNase inhibitor [Toyobo], 1 tablet/10 ml of Complete mini-protease inhibitor cocktail [Roche]). After centrifugation at 15,000 rpm for 20 min at 4°C, 50-μl aliquots of the supernatants were recovered as input samples and the remaining supernatants were precleared with 30 μl of 50% protein G-conjugated Sepharose and 1 μg of mouse normal IgG for 1 h. After centrifugation of the beads, the supernatants were immunoprecipitated with 1 μg of mouse normal IgG or anti-Flag M2 antibody (Santa Cruz Biotechnology) and 30 μl of 50% protein G-conjugated Sepharose. The beads were washed five times with RNA buffer without yeast tRNA, and RNA was isolated from the precipitants and input samples with the TRIzol reagent. The RNA was reverse transcribed as described above and subjected to the first round of PCR with JEV NS1-specific primers 5′-TCTG TCACTAGACTGGAGCA-3′ and 5′-CCAGAAACATCACCAGAAGG-3′. The PCR products were then analyzed by quantitative PCR with nested primers 5′-GAGCACTGACGAGTGTGATG-3′ and 5′-AGCGACTCTC AATCCAGTAC-3′. All values were normalized by the values for the input samples (indicated as percent input).

Cellular translational reporter assay. MEFs (2×10^5) were pretreated with 1,000 U/ml of universal type I interferon (PBL Biomedical Laboratories) for 6 h. Three types of 5′ modified luciferase mRNAs (2 μg of 5′-PPP, 5′ cap$^+$/2′-O Me$^-$, and 5′ cap$^+$/2′-O Me$^+$) were transiently transfected into MEFs using the Lipofectamine 2000 reagent (Invitrogen) according to the manufacturer's instructions. At 6 h after the transfection, RNA was isolated and analyzed for the quantity of the luciferase mRNAs (*luc2*). The luciferase activities of whole-cell lysates were measured using a dual-luciferase reporter assay system (Promega). The numbers of relative light units (RLU) were normalized by the concentrations of proteins determined by use of a bicinchoninic acid protein assay kit (Thermo Scientific).

Statistical analysis. Statistical analyses were conducted on each independent data set. An unpaired Student's *t* test was used to determine the statistical significance of differences in the experimental data. *P* values of <0.05 were considered to indicate statistical significance.

RESULTS

***Ifit1*$^{-/-}$ cells fail to restrict the replication of a mutant JEV lacking 2′-O MTase activity.** Previous analysis of the flavivirus West Nile virus (WNV) 2′-O MTase revealed residues in NS5 (K61, D146, K182, and E218) that were essential for its biochemical activity (8). A WNV mutant (E218A) lacking 2′-O MTase activity was attenuated in mouse MEFs and macrophages but showed enhanced replication in *Ifit1*$^{-/-}$ cells (13, 15). As NS5 is a highly conserved protein in flaviviruses, the four residues integral to the 2′-O MTase activity are identical in WNV and JEV (Fig. 1A). Replacement of lysine 61 by alanine in the JEV NS5 MTase domain (JEV K61A) abolished the JEV 2′-O MTase activity *in vitro* (Fig. 1B). We generated *Ifit1*$^{-/-}$ mice (Fig. 2A to C) and infected MEFs with JEV WT and JEV K61A strains (Fig. 3A). The JEV WT replicated equivalently in wild-type and *Ifit1*$^{-/-}$ MEFs. In comparison, the production of the JEV K61A mutant was decreased in wild-type MEFs, suggesting that 2′-O MTase activity is required for JEV replication. Consistent with this and analogous studies with an WNV E218A strain (13), replication of the JEV K61A strain was enhanced (approximately 173-fold increased at 4 days postinfection; $P < 0.05$) in *Ifit1*$^{-/-}$ MEFs compared with wild-type MEFs. We also infected peritoneal macrophages with JEV WT and JEV K61A strains (Fig. 3B). Similar to the results obtained with MEFs, replication of the JEV WT was similarly observed in wild-type and *Ifit1*$^{-/-}$ macrophages. However, replication of the JEV K61A mutant was severely decreased in wild-type but not *Ifit1*$^{-/-}$ macrophages, and the virus was not detected at 4 days postinfection in wild-type cells. For further confirmation, we analyzed virus RNA accumulation at 4 days postinfection (Fig. 3C and D). Whereas RNA levels of JEV WT were similar in wild-type and *Ifit1*$^{-/-}$ MEFs, those of the JEV K61A mutant were markedly

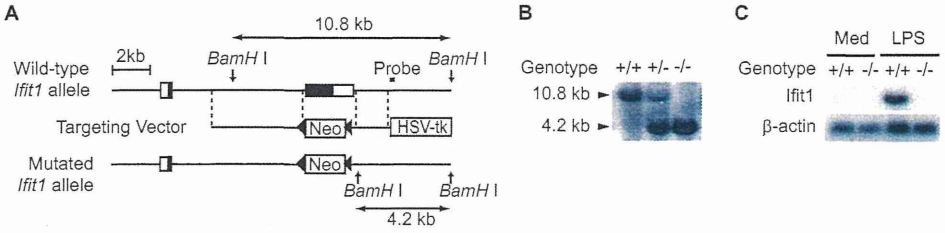

FIG 2 Generation of *Ifit1*$^{-/-}$ mice. (A) Schematic representation of the *Ifit1* gene-targeting strategies. Solid boxes, coding regions of the *Ifit1* gene; open boxes, untranslated regions; Neo and HSV tk, a neomycin-resistance gene cassette and a herpes simplex virus thymidine kinase gene, respectively. The positions of the probe and restriction enzyme site for Southern blotting are shown. (B) Genomic DNA was isolated from the tails of wild-type (+/+), heterozygous (+/-), and homozygous (−/−) *Ifit1* mutant mice. A Southern blot analysis performed after digestion of the genomic DNA with BamHI shows the correct targeting of the locus. (C) Peritoneal exudative macrophages were harvested from wild-type (+/+) or *Ifit1*-deficient (−/−) mice. Total RNA (10 μg) was blotted onto a nylon membrane, and Ifit1 and β-actin mRNA expression was detected by Northern blot analysis with the respective cDNA probes. LPS lanes, cells stimulated with 100 ng/ml of lipopolysaccharide for 4 h to induce endogenous Ifit1 expression; Med lanes, cells treated with medium alone.

higher (approximately 13-fold; $P < 0.05$) in *Ifit1*$^{-/-}$ MEFs than in wild-type MEFs. To further corroborate these findings, we reintroduced the *Ifit1* gene into *Ifit1*$^{-/-}$ MEFs using a retrovirus vector. Replication of the JEV K61A mutant was considerably suppressed (approximately 4-fold; $P < 0.05$) by ectopic Ifit1 expression in *Ifit1*$^{-/-}$ MEFs (Fig. 3E). *Ifnb* was similarly induced in wild-type and *Ifit1*$^{-/-}$ MEFs after infection with the JEV K61A mutant, excluding the possibility that defective type I IFN production is responsible for the high sensitivity to infection with the JEV K61A mutant in *Ifit1*$^{-/-}$ cells (Fig. 3F). Thus, consistent with the findings of previous studies (13, 15), Ifit1 inhibits replication and infection of flavivirus mutants that lack 2′-O MTase activity.

Ifit1 preferentially binds to virus RNA lacking 2′-O methylation. Next, we analyzed how Ifit1 recognizes 2′-O MTase mutant

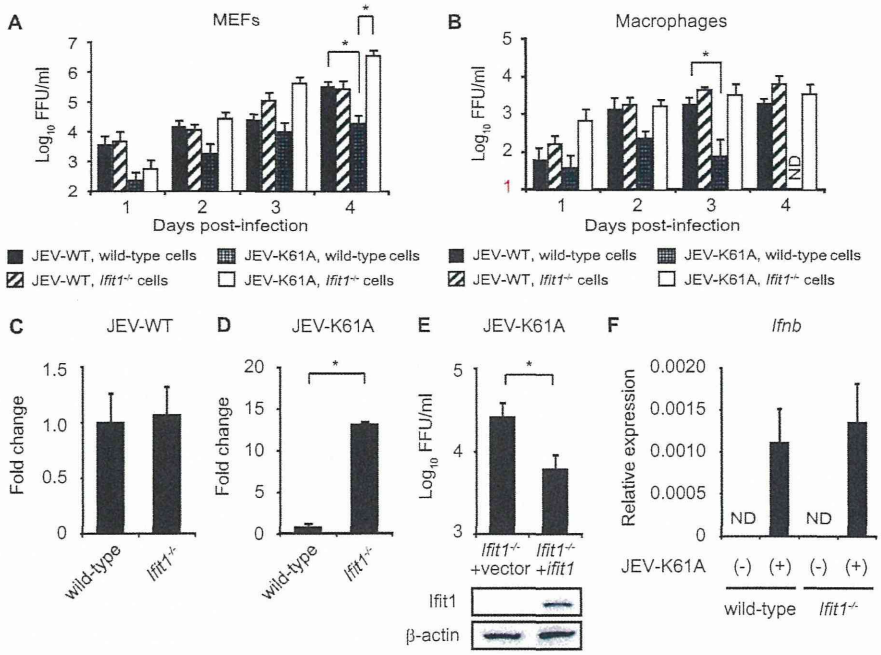

FIG 3 *Ifit1*$^{-/-}$ MEFs and macrophages fail to restrict the replication of the 2′-O MTase mutant JEV. (A, B) Culture supernatants of wild-type and *Ifit1*$^{-/-}$ MEFs (A) and macrophages (B) infected with JEV WT and the JEV K61A mutant (MOIs, 0.1 for MEFs and 0.5 for macrophages) were harvested at the indicated days postinfection. The virus titers in 1-ml supernatant aliquots were determined by focus-forming assays on Vero cells and expressed as the $\log_{10}$ number of FFU/ml. Data are shown as means ± SDs of quadruplicate samples generated from four independent experiments with statistical significance. ND, not detected. *, $P < 0.05$. (C, D) Accumulation of JEV WT (C) and the JEV K61A mutant (D) RNA in wild-type and *Ifit1*$^{-/-}$ MEFs at 4 days postinfection determined by quantitative real-time RT-PCR. JEV NS5 RNA levels were normalized to the level of host GAPDH and are expressed as the fold change in *Ifit1*$^{-/-}$ cells versus wild-type cells (value for wild type = 1). Data are representative of three independent experiments with statistical significance. *, $P < 0.05$. (E) Culture supernatants of vector-transduced (+vector) and Flag-tagged *Ifit1* gene-transduced (+*Ifit1*) *Ifit1*$^{-/-}$ MEFs infected with the JEV K61A mutant (MOI, 0.1) were harvested at 3 days postinfection. The virus titers in 1-ml supernatant aliquots were determined by focus-forming assays on Vero cells and expressed as the $\log_{10}$ number of FFU/ml. Expression of Ifit1 and β-actin determined by immunoblotting with anti-Flag or anti-β-actin antibodies is shown at the bottom. Data are representative of three independent experiments. *, $P < 0.05$. (F) Wild-type and *Ifit1*$^{-/-}$ MEFs were infected with the JEV K61A mutant (MOI, 0.1). At 4 days postinfection, cells were harvested and analyzed for *Ifnb* expression by quantitative RT-PCR. *Ifnb* RNA levels were expressed relative to those of GAPDH. ND, not detected. Data are shown as means ± SDs and are representative of data from three independent experiments.

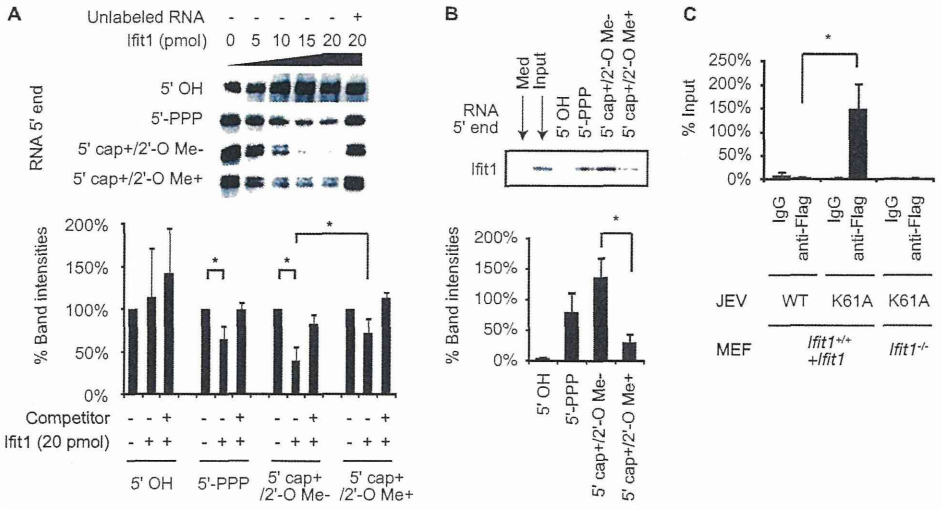

FIG 4 Ifit1 preferentially binds to virus RNA lacking 2′-O methylation. (A) Electrophoretic mobility shift of biotin-labeled RNA (JEV 5′-terminal 200 nucleotides) with recombinant Ifit1. The presence or absence of a 5′ cap and 2′-O Me of the JEV 5′-terminal 200 nucleotides is indicated. Unlabeled 5′-PPP RNA was used as a competitor. The loss of the band indicates binding of RNA and Ifit1 (top). The band intensities (in percent) calculated by ImageJ are shown at the bottom. Data are representative (top) and means ± SDs (bottom) of five independent experiments. *, $P < 0.05$. (B) Lysates from HEK293T cells transfected with HA-tagged Ifit1 were incubated with 2.5 pmol of biotin-labeled RNA. The presence or absence of a 5′ cap and 2′-O Me of the JEV 5′-terminal 200 nucleotides is indicated. 5′ OH RNA was produced by incubating *in vitro*-transcribed RNA with CIAP. RNA was incubated with streptavidin beads, and the precipitates were separated by SDS-PAGE and immunoblotted with an anti-HA antibody (top). Med and Input, samples from whole-cell lysates of empty vector- and *Ifit1*-transfected 293T cells, respectively. The percent band intensities calculated by ImageJ are shown at the bottom. Data are representative (top) and means ± SDs (bottom) of three independent experiments. *, $P < 0.05$. (C) MEFs stably expressing Ifit1 (*Ifit1*$^{+/+}$ + *Ifit1*) or *Ifit1*$^{-/-}$ MEFs were infected with JEV WT or the JEV K61A mutant at an MOI of 1.0. The cells were harvested after 24 h, and JEV RNA/Ifit1-binding complexes were immunoprecipitated with a mouse anti-Flag antibody or mouse IgG. The immunoprecipitated RNA was analyzed by nested RT-PCR using primers that detect the JEV NS1 gene. Each value was normalized by the value for the input (indicated in percent). Data are means ± SDs of three independent experiments. *, $P < 0.05$.

viruses. While recombinant IFIT1 reportedly binds to 5′-PPP RNA (32), the mRNA of the JEV K61A mutant has a 5′ m7G cap but lacks 2′-O methylation (5′ cap$^+$/2′-O Me$^-$). We examined whether Ifit1 can also interact directly with 5′ cap$^+$/2′-O Me$^-$ RNA using electrophoretic mobility shift assays. Consistent with a previous report (32), bands of 5′-PPP RNA but not RNA lacking phosphate at the 5′ end (5′ OH) were diminished after addition of recombinant Ifit1 (Fig. 4A). Furthermore, Ifit1 blocked the electrophoretic mobility of the 5′ cap$^+$/2′-O Me$^-$ RNA. However, this effect was rescued by exogenous addition *in vitro* of 2′-O methylation (5′ cap$^+$/2′-O Me$^+$). The efficient binding of Ifit1 to 5′ cap$^+$/2′-O Me$^-$ RNA was corroborated by RNA pulldown assays (Fig. 4B). HA-tagged Ifit1 was expressed in HEK293T cells, and cell lysates were incubated with biotin-labeled *in vitro*-transcribed RNA and streptavidin-agarose. Then, binding complexes of Ifit1/RNA were analyzed by Western blotting. While Ifit1 was not pulled down with 5′ OH RNA, modest binding of Ifit1 to 5′-PPP RNA and 5′ cap$^+$/2′-O Me$^+$ RNA was observed. In comparison, the strongest Ifit1 protein signal was observed with 5′ cap$^+$/2′-O Me$^-$ RNA. These findings suggest that Ifit1 preferentially binds to 5′ capped RNA lacking 2′-O methylation.

To confirm independently that Ifit1 interacts with 5′ capped RNA lacking 2′-O methylation, we performed RNA immunoprecipitation assays using cell lysates from JEV-infected MEFs that ectopically expressed a Flag-tagged Ifit1. After immunoprecipitation with an anti-Flag antibody, the JEV mRNA was measured by nested RT-PCR analysis (Fig. 4C). JEV RNA was only marginally detected in lysates precipitated with control IgG and lysates of *Ifit1*$^{-/-}$ MEFs infected with the JEV K61A mutant, indicating the specificity of Ifit1 binding in the assay. Virus RNA in JEV K61A mutant-infected MEFs was detected at a level over 37-fold higher than that in JEV WT-infected MEFs. Taken together, these findings suggest that Ifit1 directly interacts with virus mRNA lacking 2′-O methylation.

Ifit1 selectively inhibits translation of 5′ capped 2′-O unmethylated mRNA. To examine the mechanism by which Ifit1 exerts an antiviral effect by associating with mRNA lacking 2′-O methylation, we used a luciferase translational reporter assay. Luciferase RNAs with different 5′ structures were transfected into type I IFN-primed MEFs, and total RNA and cell lysates were harvested 6 h later. Importantly, the levels of luciferase RNAs in wild-type and *Ifit1*$^{-/-}$ cells were unaffected by any of the 5′ modifications (Fig. 5A). We then analyzed the translational efficiency of the transfected RNAs by measuring the luciferase activity (Fig. 5B). As expected (1), uncapped 5′-PPP luciferase mRNA was not translated in either wild-type or *Ifit1*$^{-/-}$ MEFs. Capping of the mRNA (5′ cap$^+$/2′-O Me$^-$) increased translation in wild-type cells, although the levels were profoundly lower ($P < 0.05$) than those in *Ifit1*$^{-/-}$ cells. In comparison, addition of 2′-O methylation to the 5′ cap (5′ cap$^+$/2′-O Me$^+$) *in vitro* resulted in similar levels of translation in wild-type and *Ifit1*$^{-/-}$ MEFs. Even in MEFs that were not treated with type I IFN, similar patterns of luciferase activity were observed (Fig. 5C), indicating that slightly expressed Ifit1 might contribute to the inhibition. Taken together, our data establish that Ifit1 preferentially binds to 5′ capped mRNA lacking 2′-O methylation and inhibits its translation.

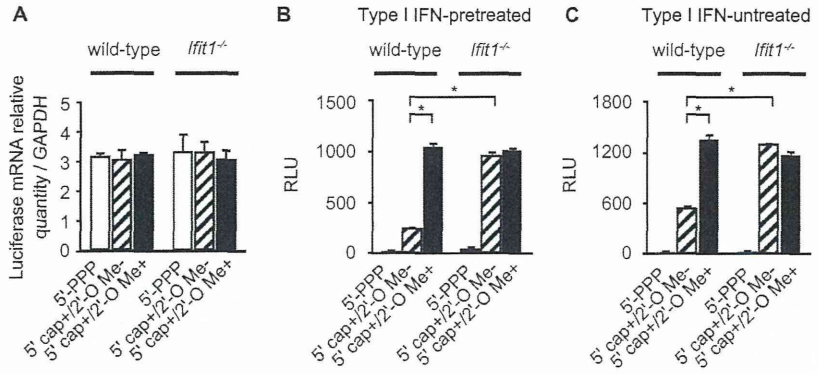

FIG 5 Ifit1 selectively inhibits the translation of mRNA lacking 2′-O methylation. (A) The luciferase RNA amounts at 6 h after RNA transfection were determined by quantitative real-time RT-PCR. The relative luciferase mRNA amounts, calculated as the amount of each transfected mRNA (*luc2*) divided by the level of GAPDH mRNA expression, are shown. The presence or absence of a 5′ cap and 2′-O Me of the introduced luciferase RNA is indicated. Data are shown as means ± SDs and are representative of three independent experiments. (B, C) Wild-type and *Ifit1*$^{-/-}$ MEFs pretreated with type I IFN (B) or untreated (C) were transiently transfected with luciferase mRNA. Luciferase activities were measured at 6 h after the transfection and are shown as relative light units (RLU). The presence or absence of a 5′ cap and 2′-O Me of the introduced luciferase RNA is indicated. Data are shown as means ± SDs of triplicate samples of the representative results. Similar results were obtained in three independent experiments. *, $P < 0.05$.

DISCUSSION

In this study, we investigated the mechanisms by which Ifit1 recognizes RNA of JEV lacking 2′-O MTase activity. Ifit1 inhibited the translation of mRNA through association with mRNA lacking 2′-O methylation.

To analyze the role of Ifit1 in 5′ cap structure-dependent antiviral responses, we generated a JEV MTase mutant. The K61, D146, K182, and E218 residues have all been shown to be essential for the MTase activity of the NS5 protein and replication of WNV (8, 11). While a WNV E218A mutant was previously used for analysis of Ifit1-mediated antiviral responses (13), in our assays, the corresponding JEV E218A mutant was severely impaired in replication in Vero cells and rapidly reverted to the wild type during cell culture, preventing its use (data not shown). A similar phenotype was observed with the WNV D146A 2′-O methylation mutant (11). However, unlike our results, it has recently been reported that a JEV E218A mutant is stable in Vero cells (39). This would be due to the different strains used in the two studies. Thus, mutation of residues that are essential for the 2′-O MTase activity of a flavivirus NS5 protein can differentially impact replication of JEV and WNV even in cells lacking type I IFN responses and IFIT1 expression.

Previous *in vitro* studies indicated that IFIT family proteins bind to several types of RNA, including 5′-PPP RNA and AU-rich double-stranded RNA (31, 32). Indeed, an analysis of the IFIT2 crystal structure indicated the presence of a positively charged RNA-binding channel (31), findings which were supported by the X-ray crystallographic structure of complexes of 5′-PPP RNA with human IFIT5 (33, 40). We also observed that Ifit1 could bind to 5′-PPP RNA. However, our biochemical analysis showed that Ifit1 bound strongly to 5′ capped RNA lacking 2′-O methylation and addition of 2′-O methylation weakened the binding of Ifit1 to the RNA. Since mRNAs of virtually all higher eukaryotes are believed to be methylated at the ribose 2′-O position (41), this modification likely serves as a molecular pattern for discriminating self from nonself.

Although it remains unclear how 2′-O methylation reduces Ifit1 binding to RNA, structural changes to the RNA at the 5′ terminus after 2′-O methylation could sterically hamper Ifit1 binding. The crystal structure of the 5′-PPP RNA/IFIT5 complex has indicated that the RNA-binding site on human IFIT5 is located in a narrow pocket, thus raising the possibility that 5′ capped and 2′-O methylated RNA cannot fit within an analogous pocket of Ifit1 due to a size limitation (33). Future structural analyses of the binding complex of 5′ capped RNA with Ifit1 will be required to reveal the precise mechanisms by which Ifit1 recognizes 5′ capped RNA lacking 2′-O methylation. Additional studies must also test whether other IFITs preferentially associate with 5′ capped RNA lacking 2′-O methylation.

Ifit1 also has an antiviral activity against several negative-stranded viruses, such as vesicular stomatitis virus (VSV) and parainfluenza virus type 5 (PIV5) (32, 42), whose mRNAs are 2′-O methylated (6, 42). In this regard, Ifit1 is supposed to have an antiviral effect independent of 2′-O methylation. Indeed, IFIT1 is able to bind 5′-PPP genomic RNA (32).

Given the previous and present findings that Ifit1 inhibits mRNA translation (23–26), our data are most consistent with a model in which Ifit1 restricts replication of viruses with 5′ capped RNA lacking 2′-O methylation through direct RNA binding and subsequent inhibition of translation. Human IFIT1 and murine Ifit1 were previously reported to interact with eIF3 to interfere with translation (23–26), and replication of hepatitis C virus, whose RNA lacks a 5′ cap, was also impaired by IFIT1 through binding to eIF3 (43). Thus, Ifit1 may associate with both eIF3 and virus mRNA to inhibit translation and infection.

The Ifit family proteins consist of several conserved members. However, Ifit1 and Ifit2 appear to have distinct antiviral activities (44). Thus, the nonredundant and redundant roles of the Ifit family proteins remain to be elucidated. Generation of mice lacking the other members or all of the Ifit family proteins will be useful to reveal the physiological functions.

ACKNOWLEDGMENTS

We thank M. S. Diamond for fruitful discussions and suggestions, T. Wakita for providing us with the JEV AT31 strain, and T. Kitamura for providing us with Plat-E cells. We also thank Y. Magota for technical assistance, C. Hidaka for excellent secretarial assistance, and members of the K. Takeda laboratory for discussions.

This work was supported by grants from the Ministry of Education, Culture, Sports, Science and Technology, the Japan Science and Technology Agency, and The Osaka Foundation for Promotion of Clinical Immunology.